Kinetic Effects of Particle-Size and Crystal Dislocation Density on the Dichromate Leaching of Chalcopyrite

L. E. MURR AND J. B. HISKEY

Relatively pure, polycrystalline samples of Golden, New Mexico and Transvaal, South Africa chalcopyrite were ground and polished to fit into a density-compatible titanium alloy sandwich assembly and shock loaded (the Golden at 1.2 GPa, the Transvaal at 18 GPa peak pressure). The recovered samples were examined in the transmission electron microscope and observed to contain roughly 10^3 and 10^4 times more dislocations respectively than the natural, unshocked materials which contained roughly 10^7 cm^{-2}. These materials were ground to three size fractions and leached in an acid-dichromate lixiviant at 50 and 70 °C (323 and 343 K). Corresponding size fractions were prepared from the unshocked material and leached for comparison; and these experiments were extended to a range of temperatures up to 90 °C (363 K) using a Bingham Canyon, Utah chalcopyrite. An unambiguous effect of dislocations was observed at the largest size fraction leached at 50 °C (323 K): the reaction rate constant increased from 1.44×10^{-3} to 1.62×10^{-3} to 2.73×10^{-3} min^{-1} for dislocation densities increasing from roughly 10^7 cm^{-2} to 10^{11} cm^{-2}. A linear relationship in the leaching rate was observed between 25 and 60 °C (298 and 333 K) and the activation energy was calculated to be approximately 12 kcal/mol (50 kJ/mol). Above 60 °C (333 K) a conspicuous rate decrease was observed. This was related to a densification of the sulfur product layer, which at 50 °C (323 K) was a loose, porous precipitate while at 90 °C (363 K) it was a continuous, tenacious, glassy coating on the chalcopyrite particles. In addition, and more importantly, the high-temperature decline in leaching rate was inferred to be associated with adsorption of Cr(VI) ion which decreases with increasing temperature. The anomalous and unpredictable behavior of chalcopyrite leached in acid-dichromate lixiviant was therefore observed to be related to variations in a surface chemisorption mechanism as well as variations in the nature of the sulfur reaction product layer. These effects also mask the influence of crystal defects and other surface-related crystallographic effects in leaching.

THE first part of any conventional ore-dressing process ideally involves the comminution of the ore to a point where each mineral grain is essentially free. This process requires large amounts of mechanical energy which, according to the early postulate of Rittinger,[1] is presumably consumed in the creation of increased surface area.[2] However, for reasons still not defined, the actual work required in grinding is sometimes several orders of magnitude larger than the energy required to produce the new surface area and the concomitant increase in crystal defects in the individual grains.

In this regard, it is well known that the grinding of ores or concentrates to small size fractions can increase reaction kinetics, *e.g.* leaching rates, in some proportion to the decrease in the mean particle size. This effect is well documented for a wide range of mineral systems. In addition, there is also a recent study by Gerlach, *et al*[3] which has attempted to relate the improvement in leaching kinetics to an increase in the lattice defects induced by grinding a chalcopyrite concentrate. In this somewhat limited work,[3] it was shown that the reaction rate (or the leaching) of a chalcopyrite concentrate could be significantly improved by an increase in what were presumed to be lattice defects created by subjecting chalcopyrite to a milling action involving a strong impact. A considerable improvement in the leaching results was obtained with ore ground in a *vibration* mill compared to those obtained with ore ground in a ball mill. Utilizing X-ray diffraction line-broadening techniques, Gerlach, *et al*[3] concluded that the longer the treatment time was in the oscillating mill, the greater was the density of crystal distortions or stored strain energy in the lattice.

More recent X-ray line-broadening observations on attritor-ground chalcopyrite by Beckstead, *et al*[4] has suggested that increased densities of crystal defects contributed insignificantly to enhanced leaching rates. These investigators concluded that leaching rate increases were dominated by increases in surface area alone.

Thus, the experimental evidence concerning the influence of crystal defects on leaching rates is inconsistent. As yet, there has been no direct evidence identifying the quantity and type of crystal defects which may be present. That is, it is unknown whether the distortional line broadening of X-ray spectra interpreted as stored strain energy is the result of increasing dislocations, twins, or stacking faults which would produce an effective grain refinement, all of which have

L. E. MURR is Professor of Metallurgical and Materials Engineering and President, New Mexico Tech Research Foundation, New Mexico Institute of Mining and Technology, Socorro, NM 87801.

J. B. HISKEY is Senior Scientist, Kennecott Minerals Company Process Technology, P. O. Box 11248, Salt Lake City, UT 84147

Manuscript submitted March 25, 1980.

ISSN 0360-2141/81/0611-0255$00.75/0

been recently shown to occur in natural chalcopyrite ($CuFeS_2$).[5] There have been no attempts to systematically increase the density of specific crystal lattice defects such as dislocations, separate from the distortional features associated with comminution, and to leach specific size fractions containing such variations in defect densities. Furthermore, the detailed nature of surfaces created by various comminution techniques has not been studied.

It was the purpose of this investigation to address these shortcomings. In particular, size fractions of chalcopyrite ($CuFeS_2$), were produced which contained specific dislocation densities which could be confirmed by direct observations of representative thin sections in the transmission electron microscope.[5] These Well-characterized size fractions were then leached along with identical but undeformed size fractions for comparison, and the rate of leaching correlated with the dislocation density. The dislocation density was generated and varied by subjecting relatively pure, polycrystalline chalcopyrite to well-defined, high-pressure shock waves. The shock wave amplitudes were varied over a range suitable to achieve variations in residual dislocation densities, without altering the initial grain size or grain morphology, and also allowing for the recovery of the shock-deformed material.

EXPERIMENTAL

Chalcopyrite Shock Deformation to Achieve Increased Dislocation Densities

It is well known that the controlled shock deformation of metals, alloys, and other materials and minerals[6–10] can produce residual defects which increase in concentration with an increase in the shock pressure at constant pulse duration. When properly initiated, a shock wave can be made to propagate through a material to produce crystal defects, principally dislocations, with little or no residual plastic strain and negligible grain refinement, distortion, or rotation in polycrystalline materials. This unique method of controlling the defect microstructure affords the opportunity to study the effects of increasing dislocation density on kinetic responses of a material without introducing variations in grain size or grain structure.

In the present experiments, samples of polycrystalline chalcopyrite from Golden, New Mexico and Transvaal, South Africa were used. These samples are described in detail elsewhere.[5] The grain size was 0.3 to 0.5 cm. Specimens were cut into 0.3 cm thick coupons, several centimeters on a side, using a diamond saw. Several coupons were cut 1.5 cm on a side and polished on all faces using standard metallographic techniques. A series of alumina powder (grit) sizes, ending with a 0.6 μm powder was employed.

The polished samples were placed in density—compatible (4.2 g/cm^3) Ti-Al-V (6 pct Al, 4 pct V) alloy sandwiches as shown schematically in Fig. 1. The cover-plate shown in Fig. 1 was then machined to the same finish and pinned to the assembly with Ti-6Al-4V dowel pins (0.3 mm diam) using a 1 kg force press-fit; and then finally lapped and polished on all sides. This sandwich (Fig. 1) was then either mounted on an aluminum projectile which impacted a stainless steel target in a 2 in. (50.8 mm) diam gas gun at Los Alamos Scientific Laboratory, or impacted directly with an explosively-driven stainless steel flyer plate as shown schematically in Fig. 2.[6]

In the gas gun experiments, a projectile velocity of 769 ms^{-1} (2500 ft. s^{-1}) was achieved in a facility described in detail by Frantz and Hecker.[11] From momentum considerations, the chalcopyrite specimen was subjected to a shock pressure calculated to be of the order of 1.2 GPa (12 k bars).[12] The sandwich assembly was recovered intact in a catcher placed beyond the impact point of the gun tube. The Golden, New Mexico chalcopyrite was employed in the gas gun experiments.

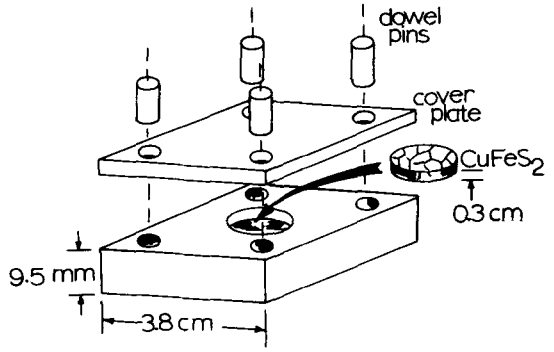

Fig. 1—Schematic view of the placement of chalcopyrite samples in density-compatible Ti-6Al-4V alloy sandwich assemblies for shock deformation (Transvaal, South Africa Chalcopyrite sample). All assembly pieces shown were the Ti-alloy.

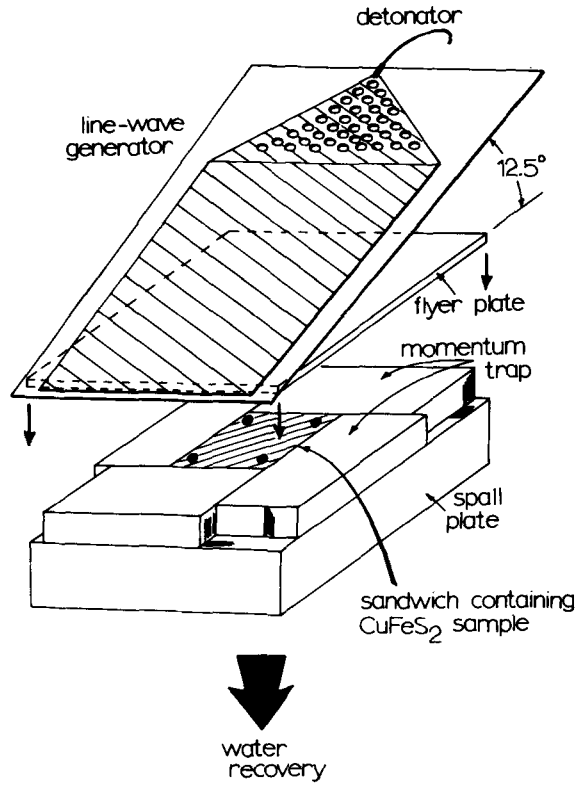

Fig. 2—Schematic arrangement for the explosive shock-loading experiment. The sandwich shown corresponds to Fig. 1.

A peak pressure of approximately 18 GPa (at a pulse duration of 2 μs) was achieved within the Fig. 1 sandwich when explosively loaded as illustrated in Fig. 2, and described in detail previously.[13] The chalcopyrite disc (Fig. 1) was retrieved following the shock event by prying the cover plate from the sandwich base. The Transvaal, South Africa chalcopyrite was employed in the high-pressure, explosive shock-loading experiments.

Dislocation Density and X-ray Line-Broadening Measurements

Small pieces of crushed and previously undeformed Golden, New Mexico and Transvaal, S.A. chalcopyrite were floated on water or blown upon white cardboard illuminated with an intense light source to show very tiny, flat specimens which could be picked up using a fine, vacuum tweezer, and placed between two, 200 mesh electron microscope screen grids for examination in the transmission electron microscope as previously described by Murr and Lerner.[5] This technique was also utilized in examining the deformed materials and comparing the electron microscope images with those of the undeformed chalcopyrite. Dislocations were readily identified as shown previously, and dislocation densities were measured in a number of samples of each material (deformed and undeformed) using the standard, statistical methods; primarily the Ham method.[14] The transmission electron microscopy was performed on a Hitachi Perkin-Elmer H.U. 200F electron microscope operating at 200 kV, and employing a goniometer-tilt stage.

Powder specimens of each of the undeformed chalcopyrites and the deformed materials of the same mesh size ($-200 + 270$ or 200×270) were examined both by slow-scan X-ray diffractometry and by the Debye-Scherer powder method in a General Electric XRD-5 X-ray unit utilizing iron $K\alpha$ radiation. Comparisons were made of the (112) reflections for all materials and line broadening was compared by considering the RMS (0.707 maximum peak height from background) peak widths.

Representative samples of materials at several size fractions were examined in the scanning electron microscope to determine the existence of surface-related cracks, or of differences in the surface topography (corresponding to serious surface area differences in a particular size range). Cracks were rarely observed (at magnifications up to 10,000 times) and the surface structures were very similar. The shock-loaded materials were, however, somewhat "smoother" indicative of perhaps a preponderance of cleavage-like fractures. This, it seems, would effectively decrease the surface area of the shocked samples. However, as we note later, this did not influence the results adversely.

Leaching of Deformed and Undeformed Chalcopyrite Size Fractions

The chalcopyrite samples used in this investigation represent three varieties: a massive Transvaal, South Africa sample, large crystals from the Golden Mines, Golden, New Mexico, and a high grade sample from Bingham Canyon, Utah. A small amount of quartz was the only impurity associated with the Transvaal and Golden Samples. The Bingham Canyon material was crushed, ground, and sized to $-100 + 150$ mesh. This size fraction was passed through a magnetic separator to remove pyrite and quartz. The upgrade sample confirmed 92 pct $CuFeS_2$.

Size samples of the Transvaal and Golden chalcopyrite were prepared fresh for this study. However, the $-100 + 150$ mesh Bingham Canyon sample was prepared about 9 years prior. Surface oxidation was removed from the Bingham Canyon sample by boiling a suspension in 1 M H_2SO_4 for approximately 5 min. It was then washed with distilled-deionized water. Drying was performed by rinsing with ethanol and ethyl ether, with final drying under vacuum.

Because of the limited quantity of Transvaal and Golden shock deformed sample material available, a rapid leaching of small sample sizes was desired. After some preliminary studies were conducted, a dichromate leach was selected because the quantity of solubilized iron and copper could be readily measured even after relatively short reaction times, (minutes) utilizing atomic absorption spectrometry.

Three different size fractions were utilized in the shocked chalcopyrite (Golden and Transvaal) leaching experiments: $-48 + 65$ mesh; $-100 + 150$ mesh; and $-200 + 270$ mesh. The samples were ground to size using a mortar and pestle. Individual leaching experiments were performed on each size range for each material: Golden, New Mexico chalcopyrite—undeformed and deformed (1.2 GPa); Transvaal, South Africa chalcopyrite—undeformed and deformed (18 GPa). Each leach utilized 0.5 g of sample. Leaches were conducted at 50 and 70 °C (323 and 343 K) for each of the four samples and three size ranges in a stirred vessel. The leaching reaction was as follows:

$$6\,CuFeS_2 + 5\,K_2Cr_2O_7 + 35\,H_2SO_4 \rightarrow 5\,K_2SO_4 + Fe_2(SO_4)_3 + 5\,Cr_2(SO_4)_3 + 6\,CuSO_4 + 35\,H_2O + 12\,S^\circ \quad [1]$$

This is similar to the dichromate leach described previously by Shantz and Morris.[16]

Leaching tests were conducted in a 1-liter three necked pyrex distilling flask. A 500 ml volume of a sulfuric acid solution of potassium dichromate was prepared fresh for each experiment and was added to the reaction vessel. During the leaching experiments the reaction flask was immersed in a circulating, oil-filled, constant-temperature bath. The $CuFeS_2$ was added to the solution when the operating temperature had stabilized. The suspension was agitated by an overhead stirring assembly.

Distilled-deionized water and reagent grade chemicals were used to prepare the appropriate leaching solution. Samples of the leach solution, always 20 ml, were removed from the reaction vessel at various times. Necessary corrections were made for the additions by simple inventory schemes (mass balance). Precautions were employed to avoid withdrawing any solids from the leaching system. Each sample was analyzed for copper by atomic absorption spectrophotometry.

The standard experimental conditions, unless stated otherwise, were 0.05 M $K_2Cr_2O_7$, 0.5 *M* H_2SO_4, 0.5 g $CuFeS_2$, and 500 rpm. All conditions for sampling and analysis were kept constant.

RESULTS AND DISCUSSION

Dislocation Densities in Shock-Loaded Chalcopyrites

Figure 3 shows for comparison the (112) X-ray reflection peaks for the natural (unshocked or as-received) and shock-loaded Transvaal chalcopyrite respectively. The RMS peak broadenings for the unshocked materials were essentially identical while some broadening was observed with shock loading. Figure 4 shows some examples of the characteristic microstructures for the chalcopyrite samples observed in the transmission electron microscope. Figure 4 (*a*) shows primarily edge-type dislocations which meet the surface of the specimen within the circled areas. The direction of the Burgers vector (**b**) shown in Fig. 4(*a*) was determined by the $g \cdot \mathbf{b} = 0$ invisibility criterion achieved by tilting the specimen in the electron microscope.[14] Figure 4(*b*) shows a very dramatic increase in dislocation density following shock loading at 18 GPa. The dislocations in the dense arrangements shown were observed to be of a mixed character (edge and screw-types). Figure 5 summarizes the actual data extracted from Fig. 3, and measurements of a large number of samples of unshocked and shock-loaded microstructures in the Transvaal and Golden chalcopyrites similar to the examples shown in Fig. 4. The X-ray line width ratios plotted in Fig. 5 were determined by simply taking the RMS peak width for the shocked/unshocked samples shown typically in Fig. 3. It is clear from Fig. 5 that X-ray line broadening is indicative of dislocation density differences, and that the dislocation density was altered markedly and somewhat systematically by the shock-loading experiments.

Leaching Experiments

The main purpose of this research was to quantify the influence of lattice defects on the rate of leaching chalcopyrite. Figures 3 to 5 illustrate the success in achieving systematic variations in dislocation density in chalcopyrite. To accomplish this objective, the measured rate must be controlled by a surface reaction, and not limited by transport through an inhibiting reaction product layer which could mask the effect of dislocations intersecting the surface as shown in Fig. 4 (*a*).

Dislocations intersecting the specimen surface represent a small energy difference relative to the undisturbed lattice, and in the case of chalcopyrite, it will be a region of altered stoichiometry as well. Consequently, it might be expected, as assumed by other investigators, that this feature, although extremely local, could give rise to a difference in leaching kinetics. Diffusional control would conceal the effects of defect structure on the chemical reaction. For this reason, and the rapid reaction rate desired, an acid-dichromate leaching system was adopted. Dichromate ion is a strong, stable oxidizing agent known for its ability to rapidly dissolve chalcopyrite.[15,16] The extremely high equilibrium potential associated with the dichromate system will result in a proportionately high anodic mixed potential for chalcopyrite leaching. As observed by Warren,[17] a high anodic potential yields an elemental sulfur product layer which is nonprotective. Miller and Portilla,[18] during their investigation of the silver catalysed ferric sulfate leaching of chalcopyrite, observed that the elemental sulfur reaction product forms as a porous non-protective layer. They interpreted the kinetics in terms of an intermediate electrochemical reaction in the Ag_2S film. Therefore, surface reaction may control the kinetics of dichromate ion leaching. The high levels of copper extraction observed with the dichromate system eliminates analytical uncertainties and helps to establish reliable data about initial reaction rates where the reaction is attributed to surface control.

The following reactions illustrate the overall stoichiometry

$$6CuFeS_2 + 5Cr_2O^{2-} + 7OH^+ = 6Cu^{2+} + 6Fe^{3+} + 2S^\circ + 10Cr^{3+} + 35H_2O \quad [2]$$

yielding sulfur;

$$6CuFeS_2 + 17Cr_2O_7^{2-} + 142H^+ = 6Cu^{2+} + 6Fe^{3+} + 12SO_4^{2-} + 34Cr^{3+} + 71H_2O \quad [3]$$

yielding sulfate. Presumably, the actual leaching will result in the formation of both elemental sulfur and sulfate ion. To insure surface control, Reaction [3] is the preferred route of leaching (only soluble products), however it was observed that elemental sulfur remains in intimate association with the particle surface. This feature is described in detail in a later section.

Particle Size

Natural (unshocked) and shock-loaded samples in three size fractions, including −48 + 65, −100 + 150 and −200 + 270 mesh, were examined for both the Golden and Transvaal chalcopyrite at 50 and 70 °C (323 and 343 K). Typical leaching response is presented in Fig. 6, as fraction of chalcopyrite reacted *vs* time curves for natural Transvaal, 0.05 M $K_2Cr_2O_7$, 0.5 M H_2SO_4 and 70 °C (343 K). The chalcopyrite leached rapidly, with 60 pct of the copper extracted in 1 h from the −200 + 270 mesh particles. The linear kinetics observed up to approximately 0.4 fraction $CuFeS_2$ dissolved imply that the reaction is uninhibited by the sulfur layer in this region. Additional support for the contention of surface reaction control is that the magnitude of the reaction velocity constant observed at 25 °C is approximately 100 times less than values typically found for mass transfer control. The average reaction velocity constant calculated for Transvaal and Golden chalcopyrites was 1.3×10^{-4} cm/s for both samples.

Figure 7 shows a plot of the relationships between fraction reacted (α) and time (t) for a topochemical

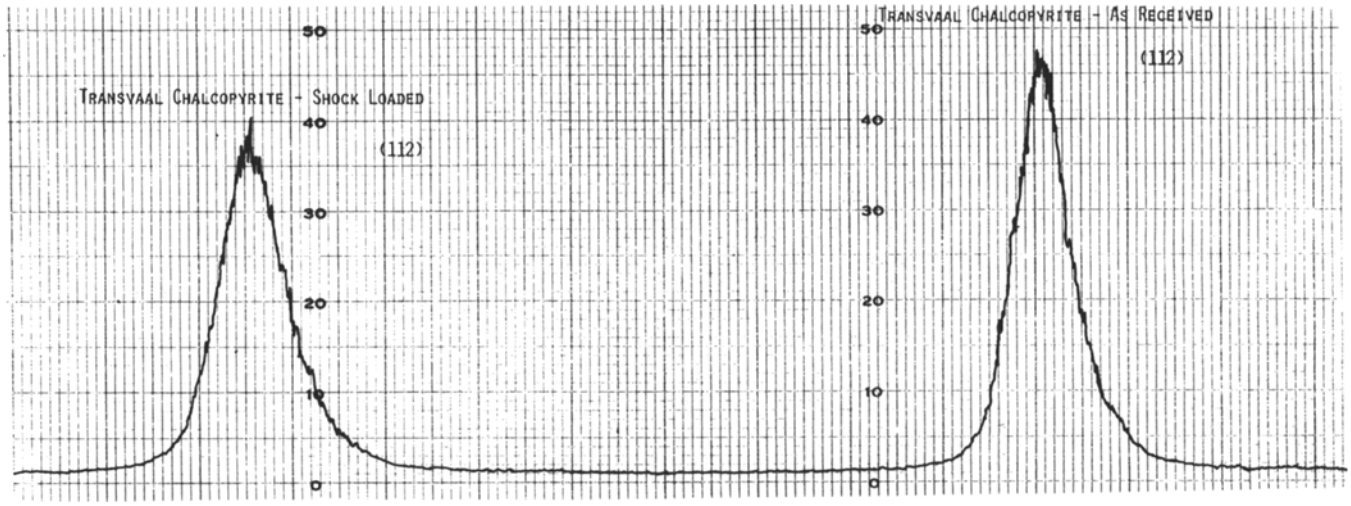

Fig. 3—X-ray diffractometer trace for the (112) reflections in the experimental chalcopyrites (− 100 + 150 size fraction). Shocked Transvaal (18 GPa) left; natural, unshocked Transvaal right.

(a)

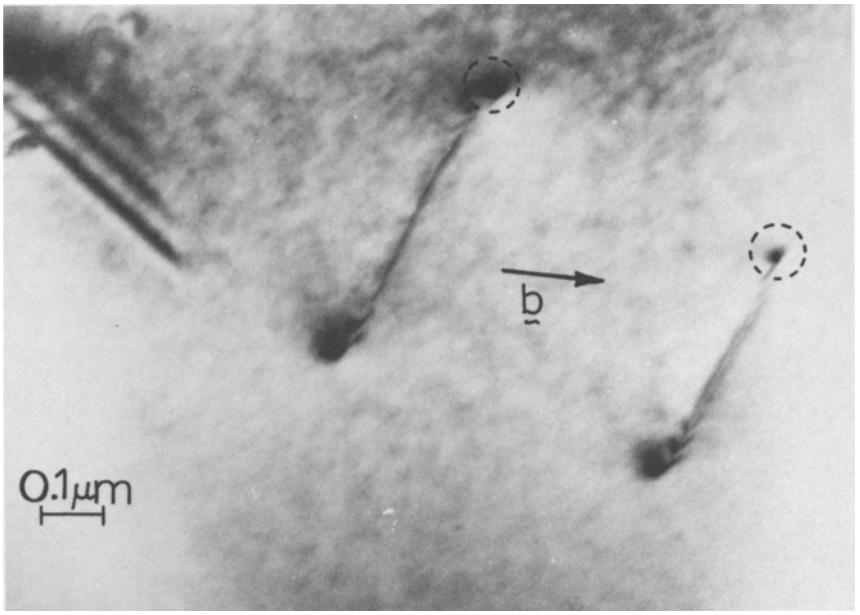

(b)

Fig. 4—Bright-field transmission electron micrographs showing dislocations in Transvaal chalcopyrite. (*a*) Natural, unshocked chalcopyrite sample. Dislocations intersecting in the surfaces of a thin section are shown in projection. The intersections with the upper surface are indicated by dotted circles. Note surface effects indicated by image broadening at the ends of the dislocation lines. (*b*) Dense dislocation arrangements typical of representative thin sections from shock-loaded (18 GPa) chalcopyrite.

reaction controlled by a surface reaction and by diffusion through a reaction product layer (assuming spherical particles)

SURFACE CONTROL:

$$1 - (1 - \alpha)^{1/3} = 2\frac{k_l C}{d_o} \quad [4]$$

DIFFUSION CONTROL:

$$1 - 2/3\alpha - (1 - \alpha)^{2/3} = \frac{8VDC}{\sigma d_o^2} t \quad [5]$$

where k_l = linear rate constant, $cm^4 mole^{-1} s^{-1}$; C = concentration of a reaching or diffusing species, moles cm^{-3}; d_o = initial particle diameter, cm; D = effective diffusion coefficient, $cm^2 s^{-1}$; V = molar volume, $cm^3 mole^{-1}$; σ = stoichiometry factor; α = fraction • $CuFeS_2$ reacted; t = time, s.

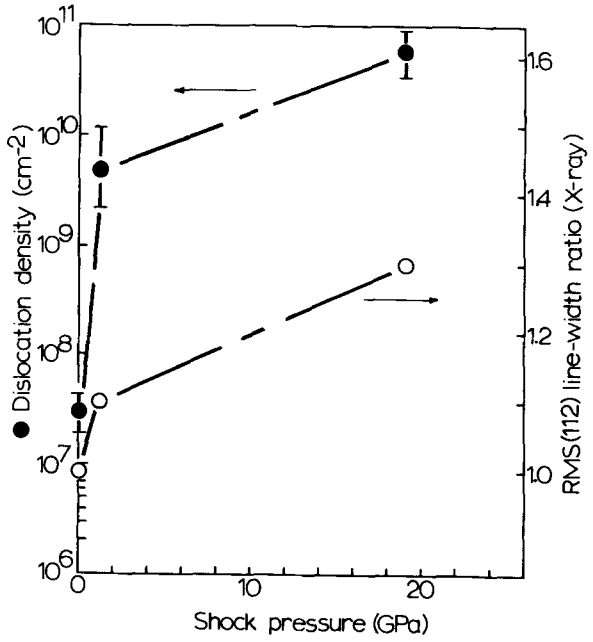

Fig. 5—Dislocation density and (112) X-ray line-width ratio *vs* shock pressure for chalcopyrite (Golden and Transvaal).

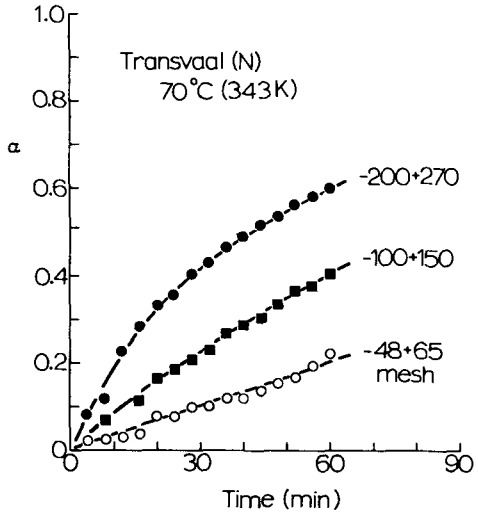

Fig. 6—Plot of fraction of copper extracted from natural (*N*), unshocked Transvaal chalcopyrite as a function of time for 0.05 M $K_2Cr_2O_7$, 0.5 M H_2SO_4, 70 °C (343 K). In the figures to follow (*N*) denotes natural or unshocked material while (*S*) will denote shock-loaded material.

The data appear to correlate well with the expression for diffusion, especially for the latter reaction period, but the plot does not yield a zero intercept as required by Eq. [5]. On the other hand, the initial leaching period fits the expression for surface control up to $\alpha \simeq 0.35$ after which a deviation from linearity is clearly apparent.

Particle size data is plotted according to Eq. [4] for Transvaal chalcopyrite samples in Fig. 8. Similar results were observed for the Golden chalcopyrite. The linear plots obtained indicate a good correlation with the surface control expression. The slopes ($k_s = 2k_l C/d_o$) for these lines should be inversely proportional to the initial particle diameter. Figure 9 is a plot of k_s *vs* $1/d_o$ for Transvaal and Golden chalcopyrites, the linear fit further justifies the application of the surface control reaction model to early stages of $CuFeS_2$ leaching of these conditions.

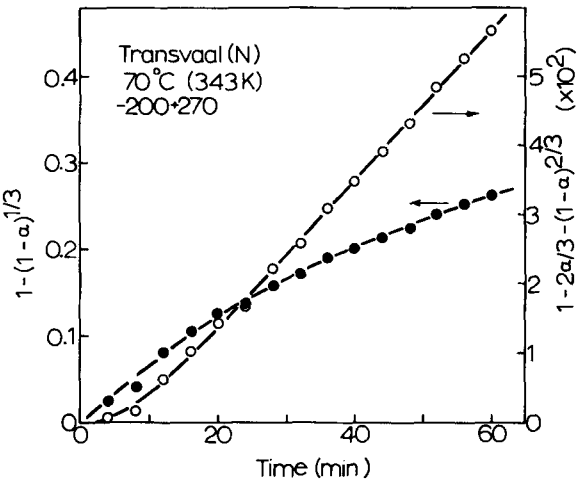

Fig. 7—Comparison of surface reaction and diffusion control relationships for α (fraction reacted) as a function of time for natural, unshocked Transvaal chalcopyrite.

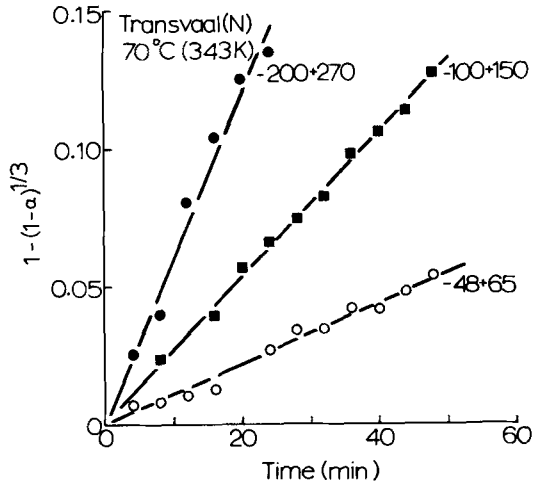

Fig. 8—Plot of $1 - (1 - \alpha)^{1/3}$ as a function of time for natural (*N*) Transvaal chalcopyrite.

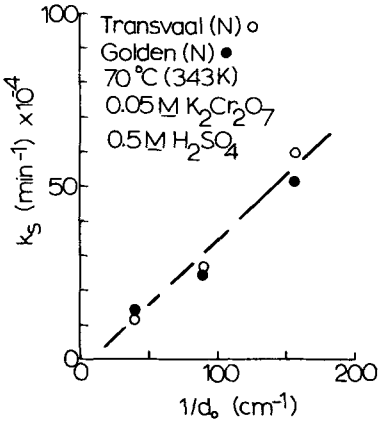

Fig. 9—Plot of the surface reaction rate constant *vs* the inverse initial particle diameter for Transvaal *N* and Golden (*N*) chalcopyrite.

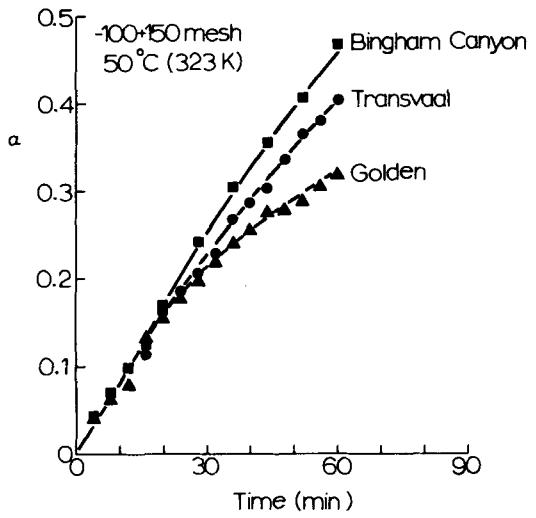

Fig. 10—Comparison of copper extraction from various chalcopyrites using 0.05 M $K_2Cr_2O_7$ and 0.5 M H_2SO_4.

Variations in Chalcopyrites

As revealed in Fig. 9 there is only a slight difference in leaching response for the Transvaal and Golden chalcopyrites at these conditions. Figure 10 shows the leaching of three varieties of − 100 + 150 mesh chalcopyrite at 0.05 M$K_2Cr_2O_4$, 0.5 MH_2SO_4, and 50 °C (323 K). These results reveal nearly identical leaching behavior for all three chalcopyrites during the early stages of leaching (up to 20 min). There are noticeable differences in leaching for longer reaction times. The Bingham Canyon sample yields the highest level of extraction, the Transvaal chalcopyrite is slightly lower, and the Golden sample shows the lowest level of extraction.

The Effect of Shock Loading and Crystal Dislocations (Dislocation Density)

When the fraction reacted (α) was plotted against time for the natural (unshocked) and shock-loaded Golden (1.2 GPa) and Transvaal (18 GPa) for each particle size distribution at 50 and 70 °C (323 and 343 K) leaching temperature, some inconsistencies were observed. All size fractions of the Golden chalcopyrite showed an increase in the rate of leaching at 50 °C (323 K) following shock loading at 1.2 GPa. However, only the largest size fraction (−48 + 65) for the Transvaal chalcopyrite showed an increase after shock loading when leached at 50 °C (323 K). At 70 °C (343 K) leaching temperature, some discrepancy was observed for the largest size fraction, while the other two size fractions showed an increase in rate following shock loading. Correspondingly, the Transvaal chalcopyrite leached at 70 °C (343 K) showed an increase in rate following shock loading for the largest and smallest particle size distributions (−48 + 65 and −200 + 270), but a decrease was observed for the medium size (− 100 + 150). Overall, therefore, the tendency was for the shock-loaded chalcopyrite to leach more rapidly.

Figure 11 shows for comparison the leaching of natural and shock-loaded chalcopyrite for two different size fractions (largest and smallest). Particularly notable is the fact that the largest *difference* occurs for the largest shock pressure as shown by the large difference

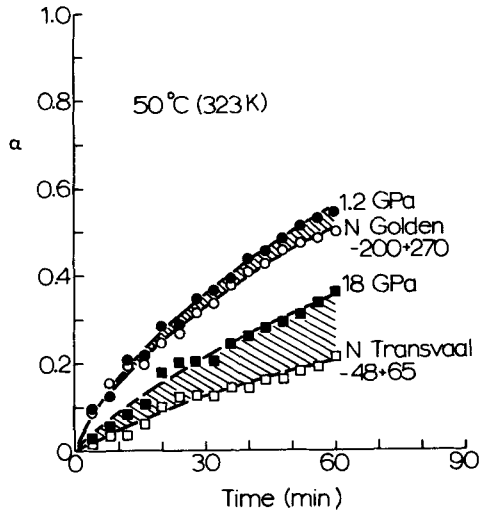

Fig. 11—Comparison of the leaching of natural (*N*) and shock-loaded (*S*) Golden and Transvaal chalcopyrite at 50 °C. (323 K)

between the shaded regimes in Fig. 11. Although the chalcopyrite regimes shown in Fig. 11 are very different, the difference is not in a direction to exaggerate the observed effects. On the contrary, the larger particle size for the larger shock pressure regime is a good comparison with the smaller particle size for the smaller shock pressure regime.

When the rate constants (k_s) in the linear region of the leaching data were determined, it was observed that the principal features apparent in Fig. 11 are supported at 50 °C (323 K) and for the larger particle size fractions. That is, Fig. 11 suggests that because the shaded region is larger for the larger shock-pressure regime, there is an apparent change in rate constant with dislocation density. This conclusion ignores the particle size difference. When the corresponding rate constants are plotted for the same particle size distribution, there is an unmistakable increase in rate constant with dislocation density as shown in Fig. 12. Table I summarizes all of the results for the shock-loading experiments for temperature and particle size regimes for

Table I. Summary of the Potassium Dichromate-Sulfuric Acid Leaching of Natural (Unshocked) and Shock-Loaded Chalcopyrites

$CuFeS_2$	Temp	Condition	Reaction Rate Constant, k_s (min^{-1}) Size Fraction, Mesh −48 + 65	−100 + 150	−200 + 270
Transvaal	50 °C (323 K)	Natural	1.44×10^{-3}	2.74×10^{-3}	—
		Shocked (18 GPa)	2.73×10^{-3}	4.00×10^{-3}	6.03×10^{-3}
	70 °C (343 K)	Natural	1.11×10^{-3}	2.61×10^{-3}	5.94×10^{-3}
		Shocked (18 GPa)	2.08×10^{-3}	2.48×10^{-3}	6.89×10^{-3}
Golden	50 °C (323 K)	Natural	1.44×10^{-3}	2.74×10^{-3}	5.84×10^{-3}
		Shocked (1.2 GPa)	1.62×10^{-3}	3.59×10^{-3}	5.87×10^{-3}
	70 °C (343 K)	Natural	1.41×10^{-3}	2.37×10^{-3}	5.12×10^{-3}
		Shocked (1.2 GPa)	1.23×10^{-3}	2.45×10^{-3}	5.31×10^{-3}

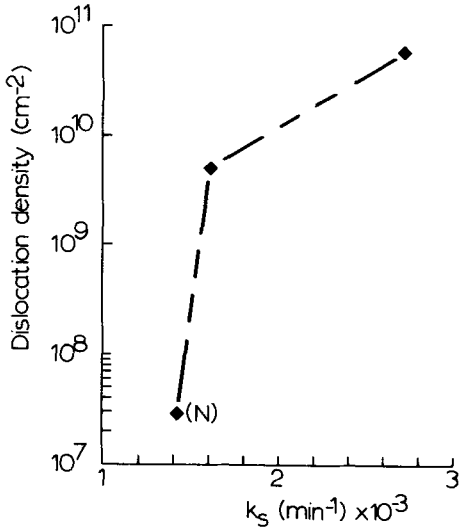

Fig. 12—Reaction rate constant, k_s, *vs* dislocation density for chalcopyrite samples.

Golden and Transvaal chalcopyrite leaching in terms of linear rate constant values, k_s. While Fig. 12 is indicative of the direct effects of dislocation density on leaching rate, Table I is indicative of the fact that shock loading (and more specifically crystal dislocations or dislocation density) has smaller or negligible effects as the particle size becomes smaller. This effect declines or becomes erratic at the higher temperature [70 °C (343 K) as compared to 50 °C (323 K)].

The variations observed in connection with the particle size-range changes can result from the increased surface-to-volume ratio for smaller particles and the decrease in the role of dislocations as a consequence of the fact that while the dislocation density (dislocation line length per unit volume —cm/cm³ or cm^{-2}) remains constant, the surface-to-volume ratio increases dramatically. In addition, shock-induced cracks, especially along grain boundaries, and so forth can be contributing at the larger particle sizes while this feature would be eliminated at smaller size fractions which are well below the grain size of the chalcopyrite. As noted earlier, examination of particles by scanning electron microscopy failed to show a preponderance of cracks. However, as noted, the shocked particles were smoother and apparently cleaved in many samples. It might be argued that the shocked samples contained slightly less surface area because of the cleavage than the unshocked, ground particles. This would simply add additional confidence to the effects of dislocations.

The Effect of Temperature

From the data summarized in Table I, it is apparent that overall the reaction is somewhat insensitive to temperature between 50 and 70 °C (323 and 343 K). In fact, the rate appears to be slightly lower at 70 °C (343 K) than at 50 °C (323 K) for these experiments. To elucidate the influence of temperature on the reaction kinetics, Bingham Canyon chalcopyrite was leached at temperatures in the range of 25 to 90 °C (298 to 363 K) because the other chalcopyrites were very limited in quantity. Figure 13 shows the leaching results for these tests. The leaching rate increases with increasing tem-

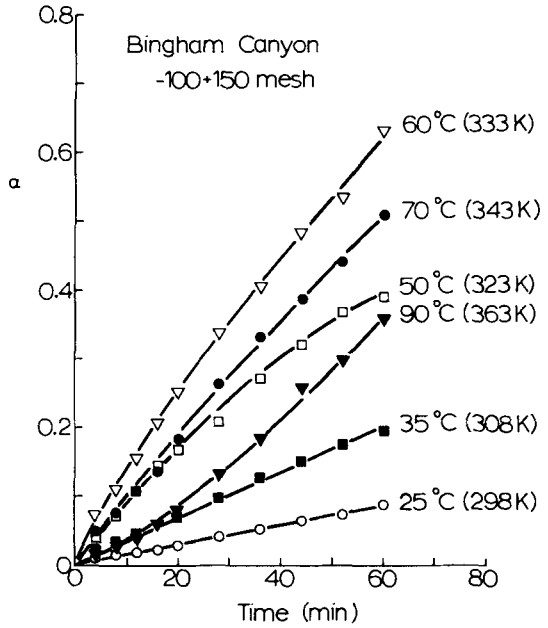

Fig. 13—Plot of fraction of copper extracted from natural, unshocked Bingham Canyon chalcopyrite as a function of time for 0.05 M $K_2Cr_2O_7$, 0.05 M H_2SO_4 − 100 + 150 size fraction.

perature up to 60 °C, but a conspicuous decrease in rate is observed from 60 to 90 °C (343 to 363 K). The surface reaction rate constants (k_s) were determined for each curve and are plotted according to an Arrhenius plot in Fig. 14. A linear relationship is observed between 25 and 60 °C (298 and 333 K) and activation energy, E_a, equal to 12 kcal/mol (50 kJ/mol) was calculated for this temperature region. The magnitude of E_a is consistent with a chemically controlled process. The leaching rate displays a maximum at approximately 60 °C (333 K).

Dutrizac[19] found a similar trend during the dissolution of zinc from an ore using an acid-ferric sulfate lixiviant. The rate of dissolution exhibited a maximum at approximately 35 °C (308 K). This unusual temperature dependence was explained in terms of the relative amounts of elemental sulfur and sulfate produced during the reaction.

Some insight was gained in regard to the elemental sulfur formed by direct observations of leached residues in the scanning electron microscope following 1 h of leaching at temperature. It was observed that at 50 °C (323 K), both the shock-loaded and natural (or unshocked) Golden and Transvaal chalcopyrite particles were covered with a very luxurious and fluffy sulfur coating which was very porous. This porous sulfur layer is very similar to the surface coating observed in the work of Miller and Portillo.[18] This sulfur coating was easily identified in the smaller particles where the fraction of the volume reacted was large, leaving a proportionately large sulfur layer. Figure 15 illustrates the elemental sulfur coating a representative number of the natural Transvaal particles in the − 100 + 150 size range leached at 50 °C (323 K). Figure 16 shows the X-ray analyses for Fig. 15(*b*) with the electron beam directed along the edge of the particle and through the sulfur coating and directly into the particle center. Figure 16 illustrates the unambiguous identification of the sulfur layer which forms.

Figure 17 shows for comparison with Fig. 15 the appearance of a − 100 + 150 mesh Transvaal chalcopyrite particle from a natural sample leached at 90 °C (363 K). It can be observed, especially on comparing Fig. 17(*b*) with Fig. 15(*b*), that at the higher temperature the sulfur layer becomes a very dense, continuous, glassy-like coating which completely envelopes the particles. The appearance of this layer is in fact nearly identical to that observed for chalcopyrite leached in acid-ferric sulfate solution at 93 °C (366 K) by Munoz, *et al.*[20] It should be noted that rhombic sulfur changes reversibly to monoclinic sulfur at 95 °C (368 K) and at 120 °C (393 K) monoclinic sulfur melts (at standard pressure). The anomalous effect of temperature observed for the leaching of the Bingham Canyon chalcopyrite can be largely attributed to the rapid densification of the sulfur product layer on the particle surfaces above 60 °C (333 K) which provides for an increasingly large diffusion barrier, with a marked change in the reaction kinetics as shown in Fig. 14. These observations provide some insight into the anomalies observed in connection with the shock-loading (crystal dislocation) effects discussed earlier in that variations in the sulfur layer integrity can give rise to variations in

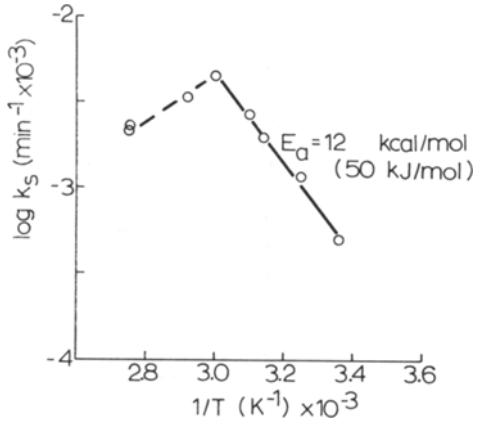

Fig. 14—Plot of log k_s *vs* reciprocal reaction temperature for Bingham Canyon chalcopyrite.

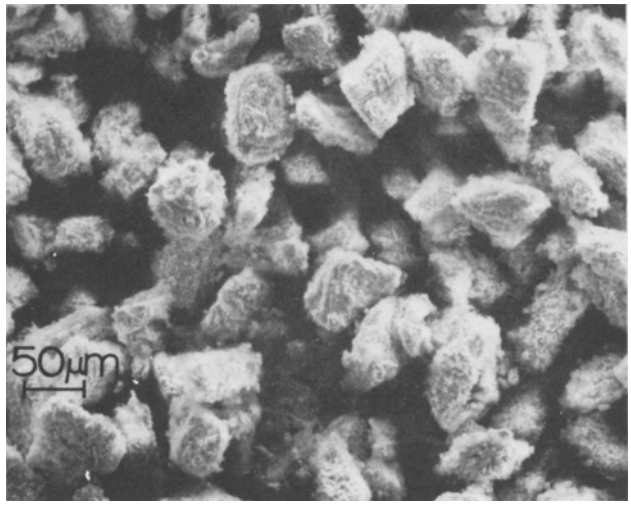

(a)

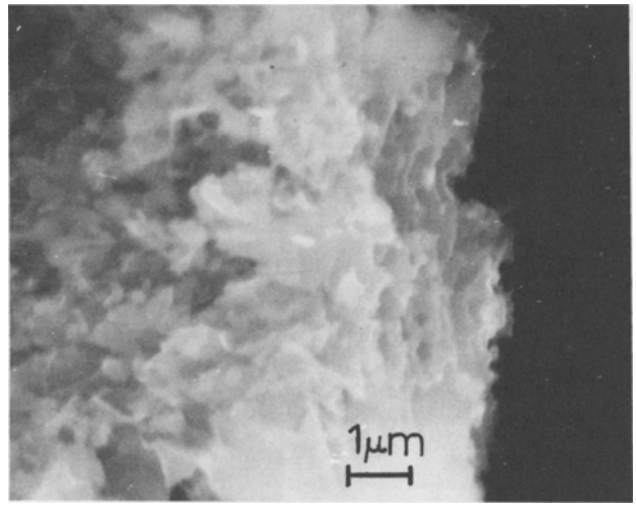

(b)

Fig. 15—Sulfur product precipitate on unshocked Transvaal chalcopyrite leached at 50 °C (323 K) for 1 h in standard dichromate lixiviant (−100 + 150 size fraction). (*a*) Particle field observed in the scanning electron microscope. (*b*) Magnified view of a particle edge showing porous, fluffy texture of sulfur layer.

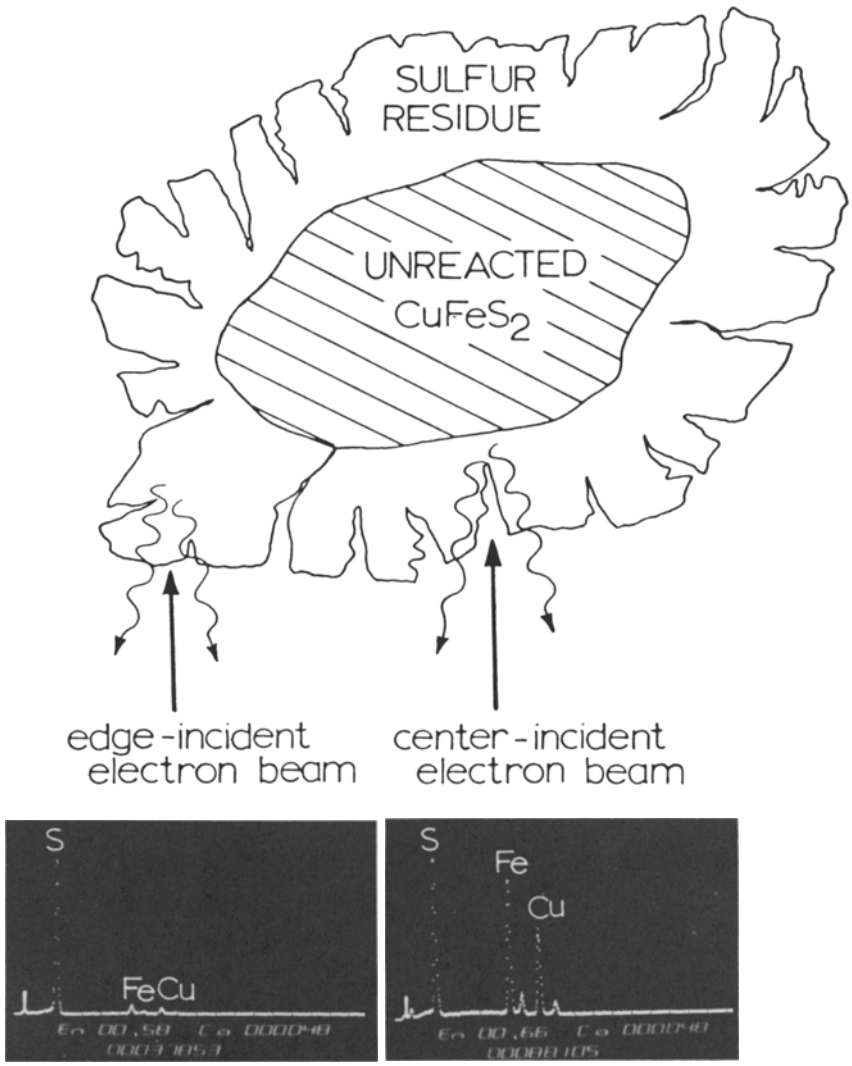

Fig. 16—Identification of sulfur product layer characteristics in the scanning electron microscope using energy dispersive X-ray spectrometry. The X-ray spectrum inserts show signal profile with beam directed as indicated.

leaching rate. Consequently, leaching at temperatures above 60 °C (333 K) may be subject to an effective masking of surface effects due to the emergence of dislocations, and the effects of dislocation density may become inconsistent or unobservable.

While the structural variations in the sulfur layer with temperature can explain the kinetic variations, they can not altogether explain the marked decline in leaching rate observed at 90 °C (363 K) as shown in Fig. 13. A similar anomaly was noted by Shantz,[15] but no attempt was made to explain it. This decline is not observed for the acid-ferric sulfate leaching of chalcopyrite recently described by Munoz, *et al*,[20] and is therefore not due entirely to the sulfur layer structure.[20] The effect must be regarded as being unique to the dichromate leach.

It would appear that the leaching of chalcopyrite with potassium dichromate in sulfuric acid involves the chemisorption of Cr(VI), $Cr_2O_7^{=}$ and/or $HCrO_4^{-}$ at the mineral surface in addition to the sulfur layer formation. Figure 18 supports this contention because it shows a response for $K_2Cr_2O_7$ *vs* k_s which is typical of an adsorption isotherm. At 25 °C (298 K), the surface is nearly saturated with Cr (VI) at 0.05 M $K_2Cr_2O_7$, the concentration used throughout these investigations. However, as the temperature increases, the concentration of the Cr (VI) species at the surface decreases because of desorption (boiling off). The critical concentration appears to be reached about 60 °C (333 K) and correspondingly above 60 °C (333 K) the sulfur layer begins to densify.

This hypothesis (Cr (VI) saturation effects) was tested by increasing the bulk concentration of $K_2Cr_2O_7$ and then studying the effect of temperature. In Fig. 19 the results of 60 °C (333 K) and 90 °C (363 K) for 0.2 M $K_2Cr_2O_7$ and 0.5 M H_2SO_4 essentially prove this because, as expected, the rate of leaching increases with increasing temperature from 60 °C to 90 °C (333 to 363 K) just as in the case of acid-ferric sulfate leaching.[20] In addition, the activation energy for this temperature range is in line with the value found between 25 °C and 60 °C at the same conditions. This feature is shown in Fig. 20. The slightly lower value for E_a noted in Fig. 20 is due in part to the inclusion of the additional experimental points in constructing the straight line. These observations indicate that not only is the sulfur layer a mitigating feature of the effects of crystal dislocations, but also in addition the selective adsorption of Cr (VI) species influences their response to leaching.

The observations described in Figs. 15 to 20 explain

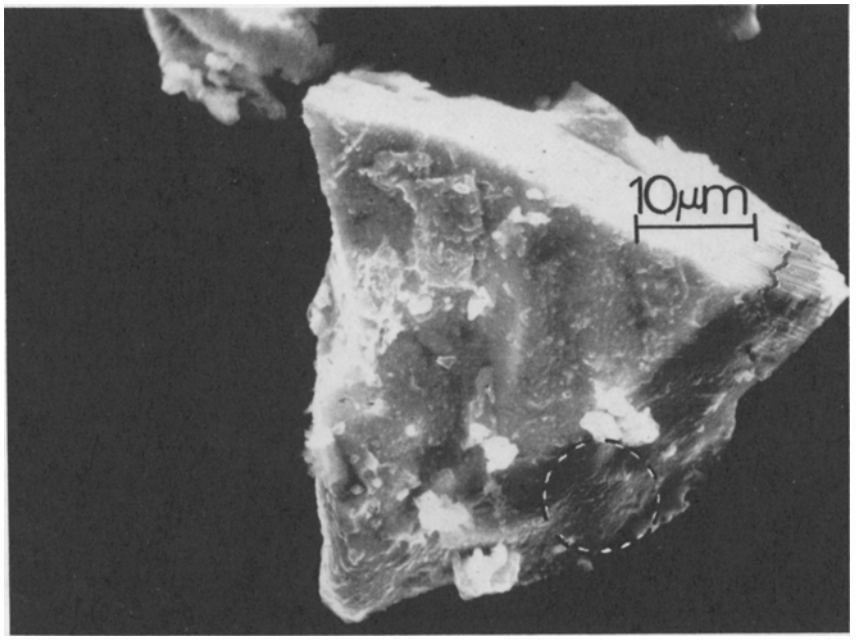

(a)

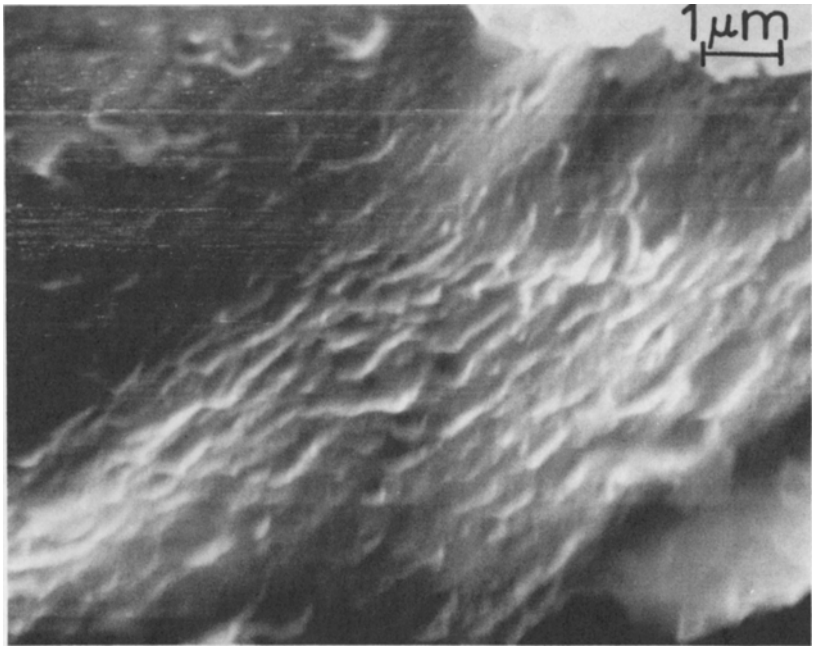

(b)

Fig. 17—Sulfur product layer on unshocked Transvaal chalcopyrite particle leached at 90 °C (363 K) for 1 h in standard dichromate lixiviant (−100 + 150 size fraction). (*a*) particle observed in the scanning electron microscope. (*b*) magnified view of region circled in (*a*) showing continuous, glassy texture of sulfur layer.

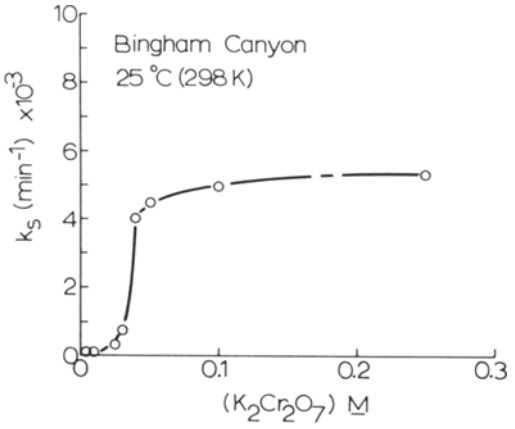

Fig. 18—Reaction rate constant (k_s) *vs* dichromate concentration for Bingham Canyon chalcopyrite.

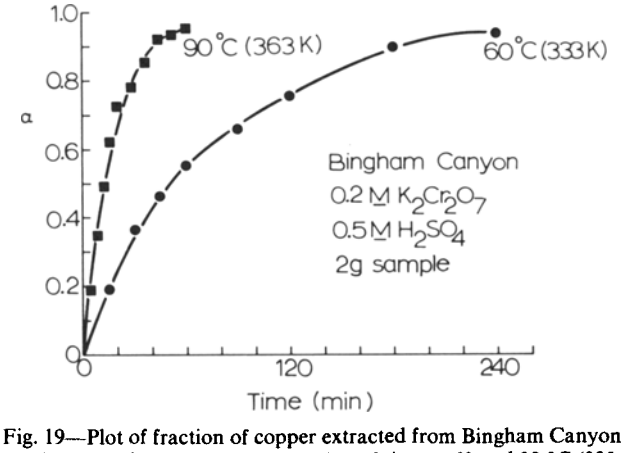

Fig. 19—Plot of fraction of copper extracted from Bingham Canyon (unshocked) chalcopyrite as a function of time at 60 and 90 °C (333 and 363 K).

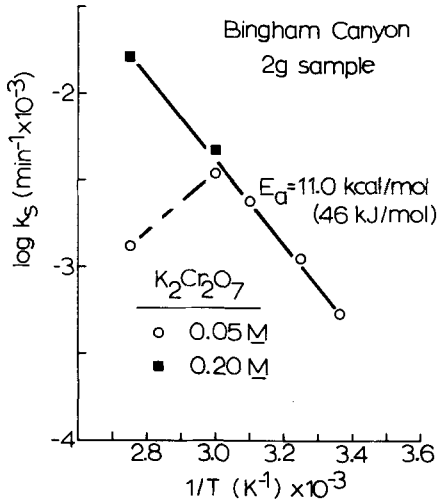

Fig. 20—Plot of log k_s *vs* reciprocal reaction temperature for Bingham Canyon chalcopyrite leached in different dichromate concentrations.

the anomalous leaching effects at high temperature in dichromate solution. They also provide for an understanding of the anomalies observed as well as the masking of the effects of crystal dislocations on the leaching kinetics of chalcopyrite particles. The fact that sensitivities begin to occur much above 60 °C (333 K) is an indication of the validity of the effects observed for the larger particle size fractions leached at 50 °C (323 K) as shown in Fig. 11 and 12, and provides strong support for the effect of dislocations even though the change in rate constant is only a factor 2 for a nearly 10^4-fold increase in dislocation density. Overall, the effects of large concentrations of crystal dislocations are small and would be expected to be erratic or undetectable when the kinetic parameters are not properly monitored or adjusted. Thus, surface adsorption of an ionic species occurs or a product layer forms which masks the effect of dislocations intersecting the mineral surface. This would occur for other precipitate formation as well, such as the formation of jarosites, and so forth, in acid-ferric sulfate leaching of chalcopyrite.

CONCLUSIONS

The shock loading of polycrystalline, natural, and relatively pure chalcopyrite (Golden and Transvaal) has provided for a regular increment of crystal dislocation density to be achieved independent of any mechanical damage due to grinding. The effect of crystal dislocations on the leaching kinetics (rate) of chalcopyrite was observed to be small but certainly detectable for the largest size fraction (−48 + 65) and lower temperature (323 K): the reaction rate constant, k_s, for these conditions increased from 1.44×10^{-3} to 1.62×10^{-3} $min^{-1}$for the unshocked Golden sample and the sample shock-loaded to 1.2 GPa, and from 1.44×10^{-3} to 2.73×10^{-3} min^{-1} for the unshocked Transvaal sample and the sample shock-loaded to 18 GPa. The dislocation densities increased by a factor of roughly 10^3 and 10^4 respectively in these ranges. Dislocation effects at small particle size fractions and higher temperature (343 K) became erratic, and effect-of-temperature experiments on Bingham Canyon chalcopyrite revealed two mitigating surface effects. One involved a somewhat systematic alteration in surface sulfur layer structure with temperature (the layer became increasingly tight with increasing temperature and at 90 °C (363 K) the layer was a glassy coating of sulfur); the other involved the inferred adsorption of Cr (VI) ions over the surface (and this effect would be dependent both upon temperature and dichromate concentration). These effects were altered in prominence with particle size fraction-changes, which increased the surface-to-volume ratio, and simultaneously altered the effects of dislocations intersecting the mineral surface. At low temperatures (298-333 K), the activation energy was calculated to be about 12 kcal/mol (50 kJ/mol).

Surface coverage either by adsorption of ionic species or reaction product precipitation has been observed to have an important influence on leaching kinetics, and adsorption of Cr (VI) in the dichromate leaching of chalcopyrite has been inferred to be principally responsible for the anomalously large decline in the leaching rate at 90 °C (363 K). Such surface effects are able to account for anomalous behavior and other erratic observations connected with a range of microstructural influences on leaching, including the possible role of different crystallographic surface orientations.

ACKNOWLEDGMENTS

This research was supported in part by the National Science Foundation (RANN Grant AER-76-03758-A01 and DAR Grant 7826167) and by the Research and Development Division of New Mexico Institute of Mining and Technology. We are grateful to Suzanne Lerner for her help with the leaching of the Golden and Transvaal chalcopyrite samples under the support of a Battelle-Sullivan Fellowship through the John D. Sullivan Center for In-Situ Mining Research. We also thank Dr. S.S. Hecker and C. Frantz for shock loading one sample in the LASL gas gun.

REFERENCES

1. T. Rosenqvist: *Principles of Extractive Metallurgy*, p. 200, McGraw-Hill Book Co., New York, 1974.
2. J. Gross and S. R. Zimmerly: *Trans. AIME*, 1930, vol. 87, pp. 35-40.
3. J. K. Gerlach, E. D. Gock, and S. K. Ghosh: "Activation and Leaching of Chalcopyrite Concentrates with Dilute Sulfuric Acid", *AIME Internat. Symp. on Hydromet.*, D. J. I. Evans and R. S. Shoemaker, eds., pp. 403-10, AIME, New York, 1972.
4. L. W. Beckstead, P. B. Munoz, J. L. Sepulveda, J. A. Herbst, J. D. Miller, F. A. Olsen and M. E. Wadsworth: "Acid Ferric Sulfate Leaching of Attritor-Ground Chalcopyrite Concentrates", *Extractive Metallurgy of Copper: Hydrometallurgy and Electrowinning*, vol. II, J. C. Yannopoulus and J. C. Agarwal, eds., chapt. 31, pp. 611-32, AIME, New York, 1976.
5. L. E. Murr and S. L. Lerner: *J. Mater. Sci.*, 1977, vol. 12, pp. 1349-54.
6. L. E. Murr and F. I. Grace: *Exptl. Mechs.*, 1979, Vol. 5, pp. 145-156.
7. W. F. Müller and U. Hornemann: *Earth Planet. Sci. Letters*, 1969, vol. 7, pp. 251-64.
8. D. Stöffler: *I. Fortshr. Mineral.* 1972, vol. 49, pp. 50-113.

9. R. W. Rohde, B. M. Butcher, J. R. Holland, and C. H. Karnes 9eds.): *Metallurgical Effects at High Strain Rates*, Plenum Press, New York, 1973.
10. L. E. Murr and K. P. Staudhammer: *Mater. Sci. Engr.*, 1975, vol. 20, pp. 35-53.
11. C. Frantz and S. S. Hecker: High-rate Mechanical Testing with the LASL Two-Inch Gun, LASL Report LA-6528, Nov., 1976.
12. R. Kinslow, ed.: *High Velocity Impact Phenomena*, Academic Press, New York, 1970.
13. L. E. Murr and S. L. Lerner: *J. Mater. Sci.*, 1978, vol. 13, pp. 2268-72.
14. L. E. Murr: *Electron Optical Applications in Materials Science*, McGraw-Hill Book Co., New York, 1970.
15. R. Shantz: Ph.D. thesis, University of Arizona, Tucson, Ariz., 1974.
16. R. Shantz and T. M. Morris: *Engr. Mining J.*, 1974, vol. 175, no. 5, pp. 71-72.
17. G. W. Warren: Ph.D. Dissertation, Dept. of Metallurgical and Fuels Engineering, University of Utah, Salt Lake City, Utah, 1978.
18. J. D. Miller and H. Q. Portillo: "Silver Catalysis in Ferric Sulfate Leaching of Chalcopyrite", XIII International Mineral Processing Congress, Warsaw, Poland, 1979.
19. J. E. Dutrizac: *CIM Bulletin*, vol. 72, No. 810, 1979, pp. 109-18.
20. P. B. Munoz, J. D. Miller, and M. E. Wadsworth: *Met. Trans. B*, 1979, vol. 10B, pp. 149-58.